Extensive Studies on π-Stacking of Poly(3-alkylthiophene-2,5-diyl)s and Poly(4-alkylthiazole-2,5-diyl)s by Optical Spectroscopy, NMR Analysis, Light Scattering Analysis, and X-ray Crystallography

Takakazu Yamamoto,*,† Dharma Komarudin,† Minoru Arai,† Bang-Lin Lee,† Hajime Suganuma,† Naoki Asakawa,‡ Yoshio Inoue,‡ Kenji Kubota,§ Shintaro Sasaki,|| Takashi Fukuda,⊥ and Hiro Matsuda⊥

Contribution from Research Laboratory of Resources Utilization, Tokyo Institute of Technology, 4259 Nagatsuta, Midori-ku, Yokohama 226, Japan, Faculty of Bioscience and Biotechnology, Tokyo Institute of Technology, 4259 Nagatsuta, Midori-ku, Yokohama 226, Japan, Faculty of Engineering, Gunma University, Tenjincyo, Kiryu 376, Japan, Japan Advanced Institute of Science and Technology, 1-1 Asahidai, Tatsunokuchi, Ishikawa 923-12, Japan, and National Institute of Materials and Chemical Research, Higashi-1-1, Tsukuba 305, Japan

Received November 11, 1997

Abstract: Stacking of poly(3-alkylthiophene)s P3RThs and poly(4-alkylthiazole)s P4RTzs has been studied. Light scattering analysis indicates that head-to-tail (HT) type HT-P3HexTh (R = *n*-C_6H_{13}) gives a degree of depolarization (ρ_v) of 0.26 in $CHCl_3$, which reveals that HT-P3HexTh takes a stiff structure even in the good solvent. Addition of CH_3OH to $CHCl_3$ solutions of HT-P3HexTh and head-to-head (HH) type HH-P4HepTz (R = *n*-C_7H_{15}) leads to π-stacking of the polymer molecules to form stable colloidal particles. The light scattering analysis of the colloidal solution of HT-P3HexTh in a 2:1 solution of $CHCl_3$ and CH_3OH reveals that HT-P3HexTh is aggregated in a parallel style. Results of filtration experiments using membranes with 0.20 and 0.02 μm pores agree with the degree of the aggregation. P3HexThs with irregular structures (P3HexTh (Fe) and P3HexTh (Ni) with HT/HH ratios of about 7/3 and 1/2, respectively) show a weaker trend to aggregate; however, P3HexTh (Fe) is considered to stack in a surface region of a stretched poly(ethylene terephthalate) PET film. A dichroism observed with the stretched PET film indicates that the $\pi-\pi^*$ absorption as well as photoluminescence of the stacked P3HexTh molecules have a transition moment along the direction of the polymer main chain. X-ray diffraction analysis of HT-P3RThs and HH-P4RTzs reveals that they take a face-to-face stacked structure with an end-to-end packing mode, except for HT-P3MeTh (R = Me). HT-P3MeTh forms a face-centered lattice with an interlayer distance of 3.51 Å. An alternative copolymer of bithiazole and 4,4′-dibutylbithiazole is packed in an interdigitation mode. At temperatures below 0 °C, the HT-P3HexTh molecules are π-stacked in $CHCl_3$, and the ^{1}H NMR spectrum shows a severe magnetic effect on the thiophene ring. Solid ^{13}C NMR data are also consistent with the π-stacking.

Introduction

π-Stacking is one of the central themes in recent organic,[1] biochemical,[2] and polymer[3−11] chemistry. Various planar aromatic molecules form the stacked structure in organic crystals (including liquid crystals),[1] DNA,[2] and polymer films,[3−12] and many of them give a plane-to-plane distance of 3.4−3.8 Å,[13] which is somewhat longer than the plane-to-plane distance of graphite (3.35 Å).

For π-conjugated polymers, self-π-stacking, especially, takes place with those polymers constituted of alkyl-substituted five-membered rings such as alkylthiophene[3−10] and alkylthiazole.[11] These polymers have been prepared by organometallic polycondensation[3,4,9,11,14−17] and oxidative polymerization[17−23] since the early 1980s,[14a,b] and recent important preparation of regioregular polymers has make it possible to investigate the

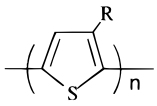

P3RTh

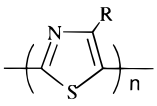

P4RTz

π-stacking of these polymers.[3−12] However, more detailed studies are needed for this interesting π-stacking.

We have been concerned with these polymers from the beginning,[11,14] and herein report results of extensive studies on the π-stacking of the polymers by optical spectroscopy, NMR

† Research Laboratory of Resources Utilization, Tokyo Institute of Technology.

‡ Faculty of Bioscience and Biotechnology, Tokyo Institute of Technology.

§ Gunma University.

|| Japan Advanced Institute of Science and Technology.

⊥ National Institute of Materials and Chemical Research.

(1) For example, see: (a) Dhirani, A.-A.; Zehner, R. W.; Hsung, R. P.; Guyot-Sionnest, P.; Sita, L. R. *J. Am. Chem. Soc*. **1996**, *118*, 3319. (b) Shetty, A. S.; Zhang, J.; Moore, J. S. *J. Am. Chem. Soc*. **1996**, *118*, 1019. (c) Graf, D. D.; Duan, R.; Campbell, J. P.; Miller, L. L.; Mann, K. R. *J. Am. Chem. Soc.* **1997**, *119*, 5888. (d) Li, W.; Fox, M. A. *J. Am. Chem. Soc*. **1996**, *118*, 11752. (e) Li, W.; Lynch, V.; Thompson, H.; Fox, M. A. *J. Am. Chem. Soc*. **1997**, *119*, 7211. (f) Munakata, M.; Wu, L. P.; Yamamoto, M.; Kuroda-sowa. T.; Maekawa, M. *J. Am. Chem. Soc*. **1996**, *118*, 3117. (g) Barbarella, G.; Zambianchi, M.; Bongini, A.; Antolini, L. *Adv. Mater*. **1992**, *4*, 282. (h) Billard, J. *Liquid Crystals of One- and Two-Dimensional Order*; Helfrich, W., Heppke, G., Eds.; Springer: Berlin, 1980; p 383. (i) Leznoff, C. C., Lever, A. B. P., Eds.; *Phthalocyanines. Properties and Applications*; VCH Publishers: New York, 1993.

S0002-7863(97)03873-0 CCC: $15.00
Published on Web 02/24/1998

analysis, light scattering analysis, and X-ray crystallography. Comparison of the behaviors of P3RTh and P4RTz provides fruitful informations concerning the self-π-stacking. Among P3RThs and P4RTzs, those with a CH_3 substituent are considered to be important, since they can easily form a coplanar π-conjugated polymer main chain due to the negligible steric repulsion caused by the CH_3 group,[11,14] in contrast to the presence of some steric repulsion caused by longer R groups. We also compare the π-stacking properties of P3RThs and P4RTzs with those of related polymers such as CT-type π-conjugated polymers.[24] Revealing the π-stacking is expected to contribute to better understanding of face-to-face $\pi-\pi$ interaction occurred with various materials and to design of polymer materials with better performance (e.g., higher electrical conductivity,[3,4] larger optical third-order nonlinear susceptibility,[11a] and ion sensing ability[3d]) which is considered to be brought about by the π-stacking.

Chart 1. Light Scattering Data of HT-P3HexTh (at 632.8 nm by He−Ne Laser) in $CHCl_3$ and Structure of the HH Unit in Regioirregular P3HexTh

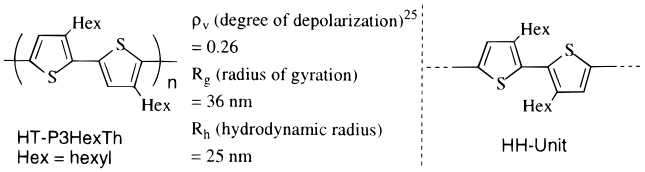

Results and Discussion

Light Scattering Analysis of HT-Type P3RTh (R = hexyl). Light scattering analysis of regioregular HT (head-to-tail)-type poly(3-hexylthiophene-2,5-diyl), HT-P3HexTh, used in this study and having a M_n value[24b] of 1.7×10^4 gives the following data in $CHCl_3$ (Chart 1).

On the other hand, a regioirregular HH (head-to-head)-rich poly(3-hexylthiophene-2,5-diyl) prepared by dehalogenative polycondensation with a Ni(0) complex,[26] P3HexTh(Ni) (HT/HH ratio = 1/2[27]), gives a much smaller ρ_v[25] value of 0.02 in $CHCl_3$. $CHCl_3$ is one of the best solvents for P3HexTh,[26b] and poly(3-dodecylthiophene-2,5-diyl) prepared by oxidative polymerization with $FeCl_3$, P3DodTh(Fe), also gives a very small ρ_v value of about 0.01 in $CHCl_3$.[26b]

(2) (a) Mathews, C. K.; van Holde, K. E. *Biochemistry*; Benjamin/Cummings Publishing: Redwood City, 1990; p 103. (b) Hall, D. B.; Barton, J. K. *J. Am. Chem. Soc.* **1997**, *119*, 5045. (c) Gilbert, M.; Claverie, P. *Molecular Associations in Biology*; Pullman, B., Ed.; Academic Press: New York, 1968; p 245. (d) Lerman, L. S. *J. Mol. Biol.* **1961**, *3*, 18. (e) Takagi, M.; Maeda, M.; Takenaka, S. *Trends Anal. Chem.* **1991**, *10*, 226. (f) Wilson, W. D.; Tanious, F. A.; Barton, H. J.; Strekowski, L.; Boykin, D. W. *J. Am. Chem. Soc.* **1989**, *111*, 5008.

(3) (a) McCullough, R. D.; Lowe, R. D. *J. Chem. Soc., Chem. Commun.* **1992**, 70. (b) McCullough, R. D.; Tristam-Nagle, S.; Williams, S. P.; Lowe, R. D.; Jayaraman, M. *J. Am. Chem. Soc.* **1993**, *115*, 4910. (c) McCullough, R. D.; Lowe, R. D.; Jayaman, M.; Anderson, D. L. *J. Org. Chem.* **1993**, *58*, 904. (d) McCullough, R. D.; Ewband, P. C.; Loewe, R. S. *J. Am. Chem. Soc.* **1997**, *119*, 633.

(4) (a) Chen, T.-A.; Rieke, R. D. *J. Am. Chem. Soc.* **1992**, *114*, 10087. (b) Chen, T.-A.; Rieke, R. D. *Synth. Met.* **1993**, *60*, 175. (c) Wu, X.; Chen, T.-A.; Rieke, R. D. *Macromolecules* **1995**, *28*, 2101. (d) Chen, T.-A.; Wu, X.; Rieke, R. D. *J. Am. Chem. Soc.* **1995**, *117*, 233.

(5) (a) Yang, C.; Orfino, F. P.; Holdcroft, S. *Macromolecules* **1996**, *29*, 6510. (b) Arroyo-Villan, M. I.; Diaz-Quijada, G. A.; Abdou, M. S. A.; Holdcroft, S. *Macromolecules* **1995**, *28*, 975.

(6) Yue, S.; Berry, G. C.; McCullough, R. D. *Macromolecules* **1996**, *29*, 933.

(7) (a) Langeveld-Voss, M. W.; Peeters, E.; Janssen, A. J.; Meijer, E. W. *Synth. Met.* **1997**, *84*, 611. (b) Delnoye, D. A. P.; Sijbesma, R. P.; Vekemans, J. A. J. M. *J. Am. Chem. Soc.* **1996**, *118*, 8717.

(8) (a) Miller, L. L.; Mann, K. R. *Acc. Chem. Res.* **1996**, *29*, 417. (b) *Chem. Eng. News* **1997**, July 28, 8.

(9) (a) Yamamoto, T. *Chem. Lett.* **1996**, 703. (b) Yamamoto, T.; Maruyama, T.; Suganuma, H.; Arai, M.; Komarudin, D.; Sasaki, S. *Chem. Lett.* **1997**, 139.

(10) (a) Märdalen, J.; Samuelsen, E.; Gautun, O. R.; Carlsen, P. H. *Solid State Commun.* **1991**, *80*, 687. (b) Märdalen, J.; Samuelsen, E. J.; Gautun, O. R.; Carlsen, P. H. *Synth. Met.* **1992**, *48*, 363. (c) Fell, H. J.; Samuelsen, E. J.; Bakken, E.; Carlsen, E.; Carlsen, P. H. J. *Synth. Met.* **1995**, *72*, 193. (d) Winokur, M. J.; Spiegel, D.; Kim, Y.; Hotta, S.; Heeger, A. J. *Synth. Met.* **1989**, *28*, C419. (e) Winokur, M. J.; Wamsley, P.; Moulton, J.; Smith, P., Heeger, A. J. *Macromolecules* **1991**, *24*, 3812. (f) Tashiro, K.; Ono, K.; Minagawa, Y.; Kobayashi, M.; Kawai, T.; Yoshino, K. *J. Polym. Sci.; Part B: Polym. Phys.* **1991**, *29*, 1223.

(11) (a) Yamamoto, T.; Suganuma, H.; Maruyama, T.; Inoue, T.; Muramatsu, Y.; Arai, M.; Komarudin, D.; Ooba, N.; Tomaru, S.; Sasaki, S.; Kubota, K. *Chem. Mater.* **1997**, *9*, 1217. (b) Yamamoto, T.; Suganuma, H.; Maruyama, T.; Kubota, K. *J. Chem. Soc., Chem. Commun.* **1995**, 1613. (c) Maruyama, T.; Suganuma, H.; Yamamoto, T. *Synth. Met.* **1995**, *74*, 183.

(12) (a) Nagao, M.; Sasaki, S.; Hayashi, T.; Uematsu, I. *Polym. Bull.* **1983**, *9*, 11. (b) Inomata, K.; Sakamaki, Y.; Nose, T.; Sasaki, S. *Polym. J.* **1996**, *28*, 992. (c) Sone, M.; Harkness, B. R.; Watanabe, J.; Yamashita, T.; Rorii, T.; Horie, K. *Polym. J.* **1993**, *25*, 997. (d) Watanabe, J.; Harkness, B. R.; Sone, M.; Ichimura, H. *Macromolecules* **1994**, *27*, 507. (e) Tashiro, K.; Hou, J.-A.; Kobayashi, M.; Inoue, T. *J. Am. Chem. Soc.* **1990**, *112*, 8273.

(13) For example, 3.4 Å for DNA[2] and various metal complexes of phthalocyanine PcH_2 (3.38 and 3.41 Å for PcNi and PcPt, respectively), and 3.6−3.8 Å for poly(3-alkylthiophene)s[3−8,10] and poly(3-alkylthiazole)s.[11]

(14) (a) Yamamoto, T.; Sanechika, K. *Chem. Ind. (London)* **1982**, 301. (b) Yamamoto, T.; Sanechika, K.; Yamamoto, A. US Pat. 1985-4521589. (c) Yamamoto, T.; Sanechika, K.; Yamamoto, A. *Bull. Chem. Soc. Jpn.* **1983**, *56*, 1497, 1503. (d) Yamamoto, T. *Prog. Polym. Sci.* **1992**, *17*, 1153; *J. Synth. Org. Chem. Jpn.* **1995**, *53*, 999. (e) Yamamoto, T.; Sanechika, K.; Yamamoto, A. *J. Polym. Sci., Polym. Lett.* **1980**, *18*, 9.

(15) Elsenbaumer, R. L.; Jen, K. Y.; Oboodi, R. *Synth. Met.* **1986**, *15*, 169.

(16) Nanos, J. I.; Kampf, J. W.; Curtis, M. D.; Gonzalez, L.; Martin, D. C. *Chem. Mater.* **1995**, *7*, 2332.

(17) (a) Czerwinski, A.; Canningham, D. D.; Amer, A.; Schrader, J. R.; Van Pham, C.; Zimmer, H.; Mark, H. B., Jr.; Pons, S. *J. Electrochem. Soc.* **1987**, *134*, 1158. (b) Czerwinski, A.; Mimmer, H.; van Pham, C.; Mark, H. B., Jr. *J. Electrochem. Soc.* **1985**, *132*, 2669.

(18) (a) Tourillon, G.; Dexpert, H.; Legarde, P. *J. Electrochem. Soc.* **1987**, *134*, 327. (b) Roncali, J.; Garnier, F. *J. Chem. Soc., Chem. Commun.* **1986**, 783. (c) Chao, S.; Wrighton, M. S. *J. Am. Chem. Soc.* **1987**, *109*, 2197. (d) Roncali, J.; Marque, P.; Garreau, R.; Garnier, F.; Lemaire, M. *Macromolecules* **1990**, *23*, 1347.

(19) Sato, M.; Tanaka, S.; Kaeriyama, K. *Synth. Met.* **1987**, *18*, 229.

(20) Sugimoto, R.; Takeda, S.; Yoshino, K. *Chem. Express* **1986**, *1*, 635.

(21) (a) Berggren, M.; Inganäs, O.; Gustalsson, G.; Rasmusson, J.; Andersson, M. R.; Hjertberg, T.; Wennerström, O. *Nature* **1994**, *372*, 444. (b) Andersson, M. R.; Selse, D.; Berggren, M.; Järvinen, H.; Hjerberg, T.; Inganäs, O.; Wennerström, O.; Österholm, J.-E. *Macromolecules* **1994**, *27*, 6503.

(22) Hotta, S.; Hosaka, T.; Soga, M.; Shimotsuma, W. *Synth. Met.* **1984**, *9*, 381.

(23) Maior, R. M. S.; Hinkelmann, K.; Eckert, H.; Wudl, F. *Macromolecules* **1990**, *23*, 1268.

(24) (a) Yamamoto, T.; Zhou, Z.-H.; Kanbara, T.; Shimura, M.; Kizu, K.; Maruyama, T.; Nakamura, Y.; Fukuda, T.; Lee, B.-L.; Ooba, N.; Tomaru, S.; Kurihara, T.; Kaino, T.; Kubota, K.; Sasaki, S. *J. Am. Chem. Soc.* **1996**, *118*, 10389. (b) $M_n = 1.7 \times 10^4$, $M_w = 2.8 \times 10^4$, and $M_z = 4.5 \times 10^4$ as estimated from GPC. The M_n value essentially agrees with that estimated from VPO (vapor pressure osmometry).

(25) (a) Kubota, K.; Urabe, H.; Tominaga, Y.; Fujime, S. *Macromolecules* **1984**, *17*, 2096. (b) Kubota, K.; Chu, B. *Biopolymers* **1983**, *22*, 1461. (c) Zero, K.; Akaroni, S. M. *Macromolecules* **1987**, *20*, 1957. (d) Huglin, M. B. *Top. Curr. Chem.* **1978**, *77*, 143. (e) $\rho_v = 3\delta^2/(5 + 4\delta^2)$, where $\delta^2 = \{(\alpha_x - \alpha_y)^2 + (\alpha_y - \alpha_z)^2 + (\alpha_z - \alpha_x)^2\}/2(\alpha_x + \alpha_y + \alpha_z)^2$ (cf. Chart 2 for α values). Under the conditions of $\alpha_x \gg \alpha_y, \alpha_z$, the ρ_v value becomes the limiting value of $^1/_3$. The observed ρ_v value seems to be for weakly stacked HT-P3HexTh molecules (likely by the side chain interaction), since the light scattering gives an approximately 6 times larger M_w than that estimated from GPC.[24b] (f) R_g ($R_g^2 = a^2/12$ for a rigid rod with a length a) is associated with M_z (Schulz, G. *J. Phys. Chem.* **1939**, *B43*, 25. Zimm, B. H. *J. Chem. Phys.* **1948**, *16*, 1099). (g) The R_g and M_w values estimated from the light scattering give a persistence length of 30 nm,[35a] which agrees with other data obtained from the light scattering measurement.

(26) (a) Miyazaki, Y.; Yamamoto, T. *Synth. Met.* **1994**, *64*, 69. (b) Yamamoto, T.; Oguro, D.; Kubota, K. *Macromolecules* **1996**, *29*, 1833.

(27) Estimated from two Th−CH_2− signals in a range of δ 2.6−2.9 ppm in the ^{1}H NMR spectrum (ref 23 and Mao, H.; Xu, B.; Holdcroft, S. *Macromolecules* **1993**, *26*, 1163).

Chart 2. Polarizability of HT-P3HexTh

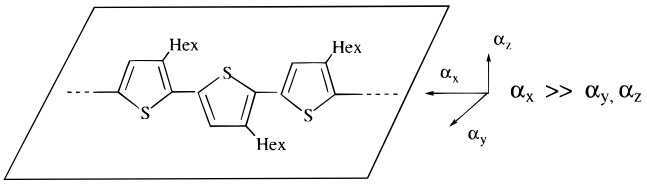

The large ρ_v value of HT-P3HexTh reveals that the HT-P3HexTh molecule takes a very stiff structure in $CHCl_3$,[25g] and the value of 0.26 indicates that the photoinduced polarizability along an axis (presumably one along the polymer chain), α_x, is much larger than the polarizability along the other two axes (Chart 2).[25e]

The ρ_v value is smaller than that of rigidly linear poly(pyridine-2,5-diyl);[28a] however, it is much larger than those (ρ_v = ca. 0.1) of all-aromatic *p*-phenylene-type linear polyamides (like Kevlar) having similar molecular weights.[25c,28b] The radius of gyration, R_g, of HT-P3HexTh roughly agrees with the molecular weight and the linear structure.[25f] The highly stiff structure of HT-P3HexTh in $CHCl_3$ suggests that a bathochromic shift observed with its colloids and films (vide infra) is not due to an increase in its stiffness in the colloids and films.

Colloidal Solution of P3HexTh (Size and Light Scattering). Despite good solubility of P3HexTh in $CHCl_3$ (solubility in solvents is summarized in the Supporting Information), it is insoluble in DMF, methanol, and ethanol. However, recently it has been reported that addition of the nonsolvent to the $CHCl_3$ solution of P3HexTh affords colloidal solutions of P3HexTh.[29,30] We have also noticed that addition of methanol to the $CHCl_3$ solution of HT-P3HexTh gives a stable colloidal solution over a wide range of $CHCl_3/CH_3OH$ ratios, and investigation of the colloidal solution yields interesting information about the stacking of the polymer.

Figure 1 compares changes of the UV−vis spectra of $CHCl_3$ solutions of various types of P3HexThs (i.e., the above-described HT-P3HexTh and P3HexTh(Ni) (HT/HH = 1/2), as well as P3HexTh(Fe) (HT/HH = 7/3) prepared by the oxidative polymerization with $FeCl_3$) on the addition of CH_3OH.

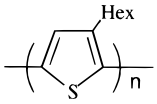

HT-P3HexTh: HT/HH = 10/0
P3HexTh (Fe): HT/HH = 7/3
P3HexTh (Ni): HT/HH = 1/2

Figure 2 exhibits UV−vis spectra of solutions after filtration of the $CHCl_3$ solution (part α in Figure 2) and the $CHCl_3$−CH_3OH colloidal solution (parts $\beta-\delta$) of HT-P3HexTh through membrane filters with pore sizes of 0.20, 0.10, and 0.02 μm, respectively. The data shown in Figure 2 directly give the size of the colloidal particle as discussed later.

UV−Vis and Light Scattering Data. As shown in part A of Figure 1, HT-P3HexTh gives the $\pi-\pi^*$ absorption band at 450 nm in $CHCl_3$, and addition of CH_3OH to the $CHCl_3$ solution of HT-P3HexTh leads to a bathochromic shift of the $\pi-\pi^*$ absorption band. The new absorption band shows splitting,[31] and the absorption peaks at 520, 560, and 610 nm agree with those of a film of HT-P3HexTh,[3−5] indicating that HT-P3HexTh takes a well-stacked structure in the colloidal particle in the $CHCl_3$−CH_3OH mixture, similar in the film.[3−10] However, the minor effect of added CH_3OH on the baseline in a range of 700−800 nm indicates that the size of the stacked particle is smaller than an order of 10^3 nm (1 μm). The solution is stable over several weeks at the concentration of HT-P3HexTh below about 15 mg L^{-1}; at a higher concentration of P3HexTh, gradual precipitation of red HT-P3HexTh is observed. Intercalation of

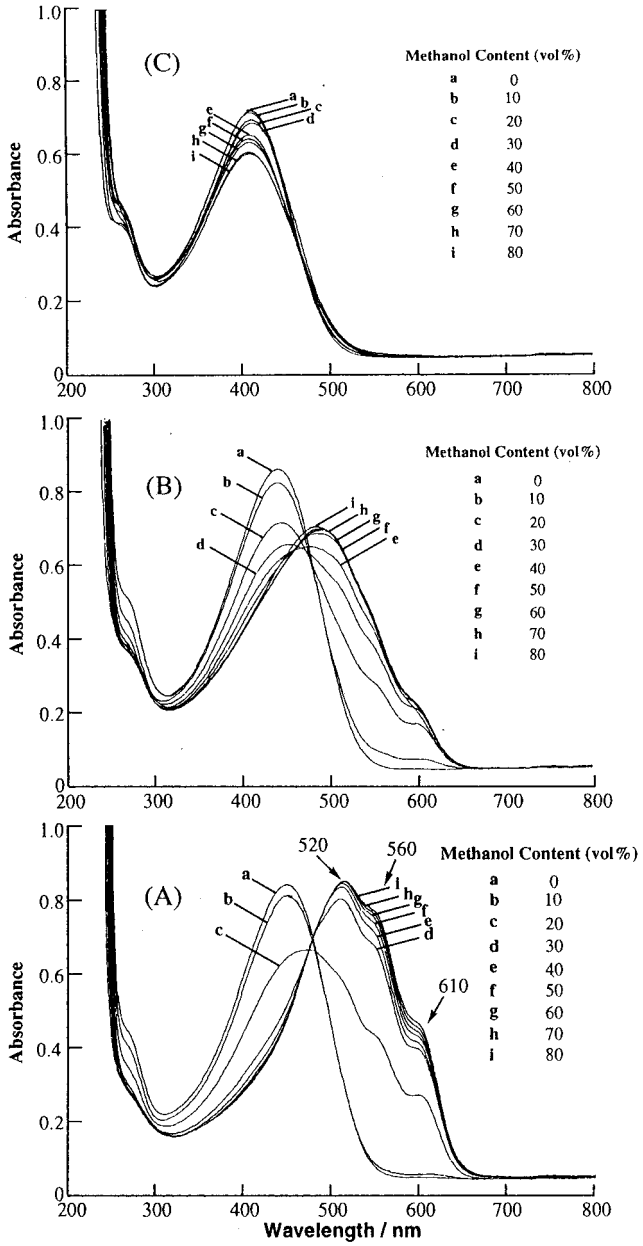

Figure 1. Changes in UV−vis spectra of $CHCl_3$ solutions of (A) HT-P3HexTh, (B) P3HexTh (Fe) (HT/HH = 7/3), and (C) P3HexTh(Ni) (HT/HH = 1/2) on addition of CH_3OH at 25 °C. [P3HexTh] = 15 mgL^{-1} or 9×10^{-5} M (monomer unit). Volume percent of CH_3OH: 0−80% for a−i as shown.

(28) (a) Yamamoto, T.; Maruyama, T.; Zhou, Z.-H.; Ito, T.; Fukuda, T.; Yoneda, Y.; Begum, F.; Ikeda, T.; Sasaki, S.; Takezoe, H.; Fukuda, A.; Kubota, K. *J. Am. Chem. Soc.* **1994**, *116*, 4832. (b) Fractionation of HT-P3HexTh by solubility[26b] gives five fractions with different molecular weights, and they give a viscosity equation of $[\eta] = 1.07 \times 10^{-6} M_n^a$ with an a value of 1.25. The a value is larger than those of P3DodTh(Fe) (a = 0.80) and P3HexTh(Ni) (a = 1.14) and is consistent with the stiffer structure of the HT-P3HexTh.

(29) Inganäs, O.; Salaneck, W. R.; Österholm, J.-E.; Laakso, J. *Synth. Met.* **1988**, *22*, 395.

(30) (a) Sandstedt, C. A.; Rieke, R. D.; Eckhardt, C. J. *Chem. Mater.* **1995**, *7*, 1057. (b) Faid, K.; Frechette, M.; Rnger, M.; Mazerolle, L.; Levesgue, I.; Leclerc, M.; Chen, T. A.; Rieke, R. D. *Chem. Mater.* **1995**, *7*, 1390.

(31) The splitting probably originate from a vibronic coupling (energy splitting = ca. 1400 cm^{-1} corresponding to the ring vibration of the thiophene ring).

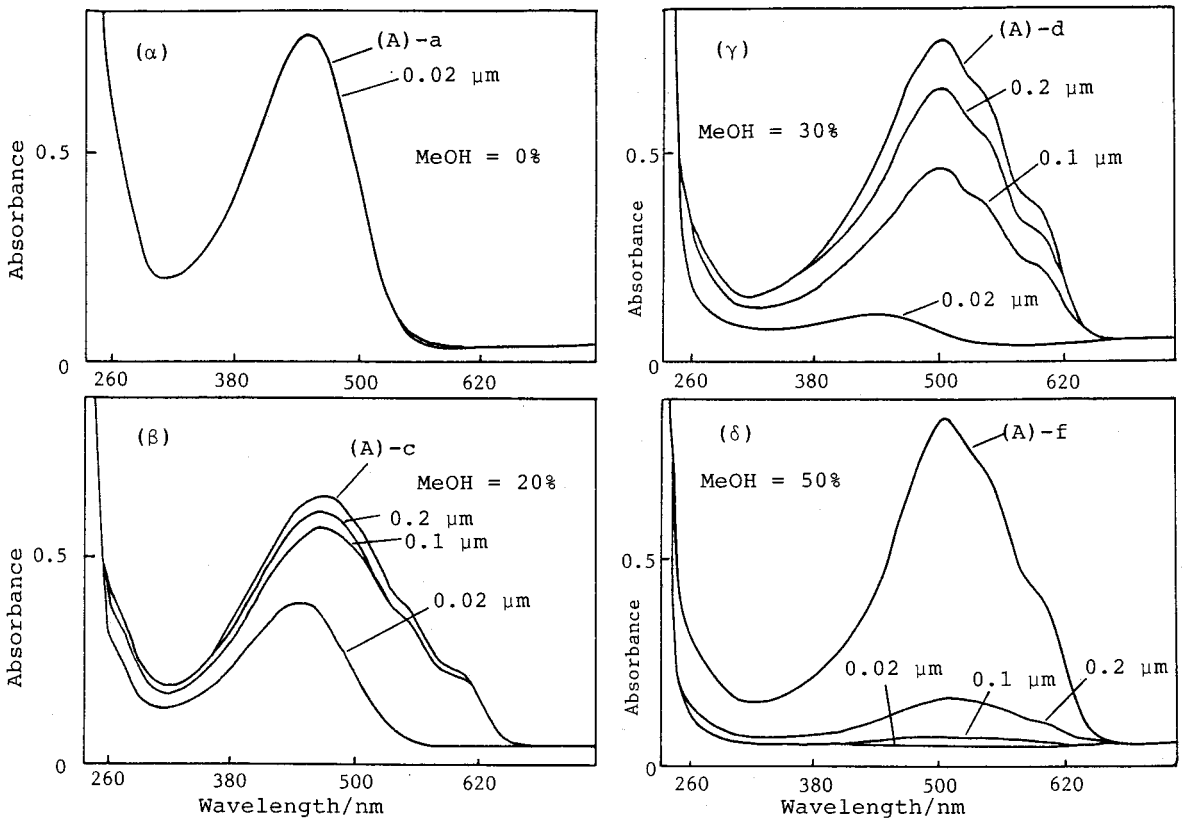

Figure 2. UV−vis spectra of the solutions of HT-P3HexTh obtained after filtration through membrane filters with pore sizes of 0.20, 0.10, and 0.02 μm. The size attached to the curves indicate the pore size of the membrane filter. Content of MeOH in the $CHCl_3$−CH_3OH mixture = 0 (α), 20 vol % (β), 30 vol % (γ), and 50 vol % (δ) in Figure 1, respectively. Concentration of HT-P3HexTh before filtration = 15 mgL^{-1}.

Chart 3. Shift of the $\pi-\pi^*$ Absorption Band

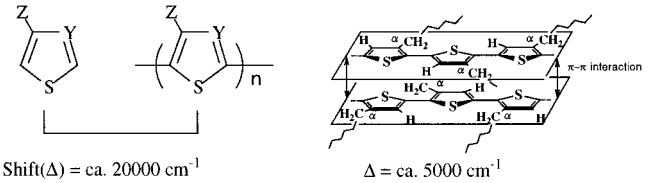

Shift(Δ) = ca. 20000 cm^{-1}
Y = CH or N; Z = H or CH_3

Δ = ca. 5000 cm^{-1}
(also for P4RTz)[11]

aromatic compounds into DNA by the π-stacking usually causes a decrease in the molar absorption coefficient of the aromatic compound;[2f] however, such a decrease in the molar absorption coefficient is not observed for HT-P3HexTh (Figure 1A). The spectrum c in Figure 1A resembles that of the intercalated aromatic compound in DNA.[2f]

P3HexTh(Fe) containing the HT unit in 70% also shows a bathochromic shift on addition of CH_3OH, as shown in part B of Figure 1. However, the degree of the stacking is apparently lower. P3HexTh(Ni) containing the HH unit as the major unit does not seem to form the stacked structure in the $CHCl_3$−CH_3OH mixtures (part C of Figure 1). Solid HT-P3HexTh is mechanically harder than solid P3HexTh(Fe) and P3HexTh-(Ni). All of these data reveal the importance of the regularly repeated HT structure for the formation of the stacked structure.

The thiophene−thiophene (as well as thiazole−thiazole) chemical bond interaction along the main chain causes the bathochromic shift of the $\pi-\pi^*$ absorption band of the monomeric compound by about 20 000 cm^{-1}.[11,14d] On the other hand, the π-stacking of the polymers (P3RThs and poly-(alkylthiazoles) P4RTzs) causes further bathochromic shift by about 4000−5000 cm^{-1} (cf. Chart 3) as depicted in Figure 1A. These data suggest that the strength of the face-to-face $\pi-\pi$ interaction due to the π-stacking roughly corresponds to 1/4 of the strength of the $\pi-\pi$ interaction along the main chain through the direct covalent bond.

As for the packing structure shown in Chart 3, the single-crystal X-ray crystallographic analysis of thiophene oligomers with substituents[1c,32] has revealed that they take the s-trans configuration between the thiophene rings, although their terminal thiophene rings sometimes deviate from coplanarity or the s-trans structure. Many of the oligomers are stacked in parallel layers, in contrast to the herringbone-type packing of nonsubstituted thiophene oligomers[33a,b] and poly(thiophene-2,5-diyl).[33c] As described later, HT-poly(3-methylthiophene-2,5-diyl), HT-P3MeTh, takes a shorter layer-to-layer distance than that of other HT-P3RThs with longer R chains and shows no bathochromic shift in the solid in contrast to the large bathchromic shift observed with other HT-P3RThs in the solid. On the basis of these facts, HT-P3HexTh is considered to take the face-to-face eclipsed-type packing mode in the stacked parallel layers, as depicted in Chart 3 and previously proposed.[4,5,10e,34] MM2 molecular mechanic calculation for two HT-type pen-

(32) (a) Barclay, T. M.; Cordes, A. W.; MacKinnon, C. D.; Oakley, R. T.; Reed, R. W. *Chem. Mater*. **1997**, *9*, 981. (b) Miller, L. L. and Yu, Y. *J. Org. Chem*. **1995**, *60*, 6813. (c) Barbarella, G.; Zambianchi, M.; Bongini, A.; Antolini, L. *Adv. Mater*. **1994**, *6*, 135. (d) Barbarella, G.; Zambianchi, M.; Marimon, M. del F. I.; Antolini, L.; Bongini, A. *Adv. Mater*. **1997**, *9*, 484. (e) Alemán, C.; Brillas, E.; Davis, A. G.; Fajarí, L.; Giró, D.; Julia, L.; Pérez, J. J.; Rius, J. *J. Org. Chem*. **1993**, *58*, 3091.

(33) (a) Horowitz, G.; Bachet, B.; Yassar, A.; Lang, P.; Demanze, F.; Fave, J.-L.; Ganier, F. *Chem. Mater*. **1995**, *7*, 1337. (b) Isz, X.; Weissbuch, I.; Kiaer, K.; Bouwman, W. G.; Als-Nielsen, J.; Palacin, S.; Ruaudel-Teixier, A.; Leiserowitz, L.; Lahav, M. *Chem. Eur. J*. **1997**, *3*, 930. (c) Brückner, S.; Porzio, W. *Makromol. Chem*. **1988**, *189*, 961.

(34) The sulfur atoms in the upper and lower layers in Chart 3 may be in the same direction, since such packing is known for oligomeric compounds[1c] and the sum (3.6 Å) of the van der Waals radius of two sulfur atoms is within the plane-to-plane distance (3.8 Å).

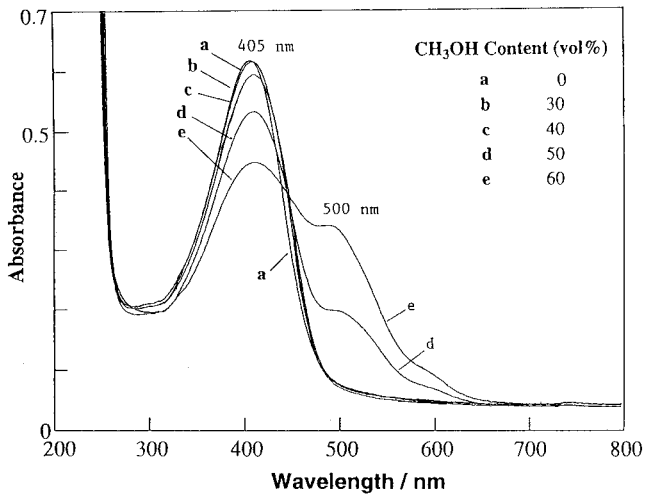

Figure 3. Changes in UV−vis spectrum of a $CHCl_3$ solution of HH-P4HepTz on addition of CH_3OH at 25 °C.

tamers of 3-hexylthiophene also supports the face-to-face packing of the two molecules with their molecular planes essentially parallel to each other without tilting. A similar molecular mechanic calculation, which is consistent with the plane-to-plane distance of 3.81 Å, has also been reported for HT-type tetramer of 3-hexylthiophene.[3b]

Addition of acetone (one of the poor solvents for P3RThs) to the $CHCl_3$ solution of HT-P3HexTh as well as addition of CH_3OH or acetone to a $CHCl_3$ solution of HT-P3DodTh (R = dodecyl) causes similar changes in the UV−vis spectrum. Aggregation of HT-P3DodTh requires addition of a larger amount of CH_3OH presumably due to a stronger solubilizing effect of the longer dodecyl chain. Use of the HT-P3HexTh in a higher concentration as well as use of a fraction of HT-P3HexTh with a higher molecular weight[28b] somewhat enhances the tendency of the polymer to aggregate (cf., the Supporting Information).

The following HH-type P4HepTz

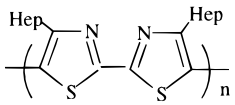

Hep = heptyl

also gives an analogous colloidal solution on addition of CH_3OH to its $CHCl_3$ solution up to 60 vol % of CH_3OH as depicted in Figure 3, and the colloidal solution gives rise to a λ_{max} at a longer wavelength (from 405 to 500 nm or $\Delta = 4700$ cm^{-1}) compared with the $CHCl_3$ solution. HH-type P4RTzs are also considered to be able to form the stacked structure in the solid (vide infra), and the degree of the stacking in their films seems to depend on preparative conditions of the film as reported by us[11a] and by Curtis and co-workers.[16] After filtration of the colloidal solution of HH-P4HepTz through the 0.02 μm membrane filter, the UV−vis spectrum exhibits only a peak at 405 nm and the new peak of the aggregated species at 500 nm completely disappears.

Size of the Colloidal Particle. As shown in part α in Figure 2, all of the HT-P3HexTh molecules in the $CHCl_3$ solution can pass through the membrane with the pore size of 0.02 μm. To the contrary, the well-stacked or aggregated HT-P3HexTh molecules in the $CHCl_3$−CH_3OH mixtures do not pass through the membrane with the pore size of 0.02 μm, as shown in parts β−δ in Figure 2. For the 80/20 mixture of $CHCl_3$ and CH_3OH, about half of the HT-P3HexTh molecules can pass through the 0.02 μm pore, and the UV−vis absorption spectrum of the filtrate agrees with that of HT-P3HexTh in $CHCl_3$. When the content of MeOH is increased to 30% (part γ), only about 10% of the HT-P3HexTh molecules can pass through the membrane, and the UV−vis absorption peak of the filtrate also agrees with that observed in $CHCl_3$.

Filtration of the 70/30 $CHCl_3/CH_3OH$ colloidal solution (part γ in Figure 2) through membranes with pore size of 0.2 and 0.1 μm reveals that (i) a part of the aggregate has a size larger than 0.1 or 0.2 μm and (ii) the UV−vis absorption pattern of the filtrate after filtration of the 0.1 μm membrane essentially agrees with that of the original solution. This result indicates that the electronic state of the stacked particle is virtually independent of its size after the size becomes larger than 0.1 μm.

When the proportion of CH_3OH is increased to 50%, essentially all of the HT-P3HexTh molecules are in the well-stacked state, as manifested from the data shown in the part δ in Figure 2.

Light scattering analysis[25] of a 67/33 $CHCl_3/CH_3OH$ colloidal solution of HT-P3HexTh (after filtration with a 0.5 μm membrane) with He−Ne laser (632.8 nm) at 25 °C gives the following data:

Chart 4. Light Scattering Data of Aggregated HT-P3HexTh

$\rho_v^{25} = 0.021$

$R_g = 42$ nm,

$R_h = 48$ nm

Scattering intensity: about 10^3 times larger compared with a $CHCl_3$ solution containing the same amount of HT-P3HexTh

Stability of the colloidal solution: the above shown four (ρ_v, Rg., etc.) values are time-independent during the measurement for 30 h.

The 10^3-times larger scattering intensity corresponds to formation of particles with a 10^3-times larger molecular weight,[35a] and only a small increase in R_g (from 36 nm of HT-P3HexTh (vide ante) to 42 nm of aggregated HT-P3HexTh) indicates that the HT-P3HexTh molecules aggregate along the main chain as depicted in Figure 4. Since the cross section of one HT-P3HexTh molecule is considered to have a dimension of about 3.8 Å × 16.4 Å,[3−8] formation of a columnar aggregate (Figure 4) gives a diameter of about 60 nm for the column and such an aggregate will not bring about substantial increase in the R_g value.[35b] The diameter of the aggregate thus estimated agree with the filtration experiments described above. To the contrary, if the HT-H3HexTh molecules are stacked together in a largely slipped style, growth of the aggregate to the direction of the *x* axis (Figure 4) will occur, and in this case, a large increase in the R_g value will be observed. Therefore, the small increase in the R_g value supports the stacking mode shown in Figure 4. That the aggregate give a larger R_h[35a−37] value than R_g indicates that the aggregate has a densely packed structure.

The large decrease in the ρ_v value (from 0.26 to 0.021; cf., Charts 1 and 4) by taking the stacked structure is reasonably explained by increasing polarizability along both the *y* and *z*

(35) (a) Flory, P. J. *Principles of Polymer Chemistry*; Cornell University Press: Ithaca, NY, 1953. (b) A column with a length *a* ($a^2 = 12R_g^2$) of 130 nm[25f] ($a = 3.5\ R_g$ = ca. 130 nm (Chart 1)) and a diameter *b* of 60 nm gives R_g of 43 nm ($R_g^2 = a^2/12 + b^2/8$) and R_h of 47 nm (Broersma, S. *J. Chem. Phys.* **1960**, *32*, 1626, 1632. Tirado, M.; de la Torre, J. G. *J. Chem. Phys.* **1979**, *71*, 2581), both values agreeing with the observed values. Since several HT-P3HexTh molecules seem to be weakly stacked in $CHCl_3$,[25e] the diameter *b* of 60 nm is estimated for stacking of about 5×10^3 molecules of FT-P3HexTh in the colloidal solution.

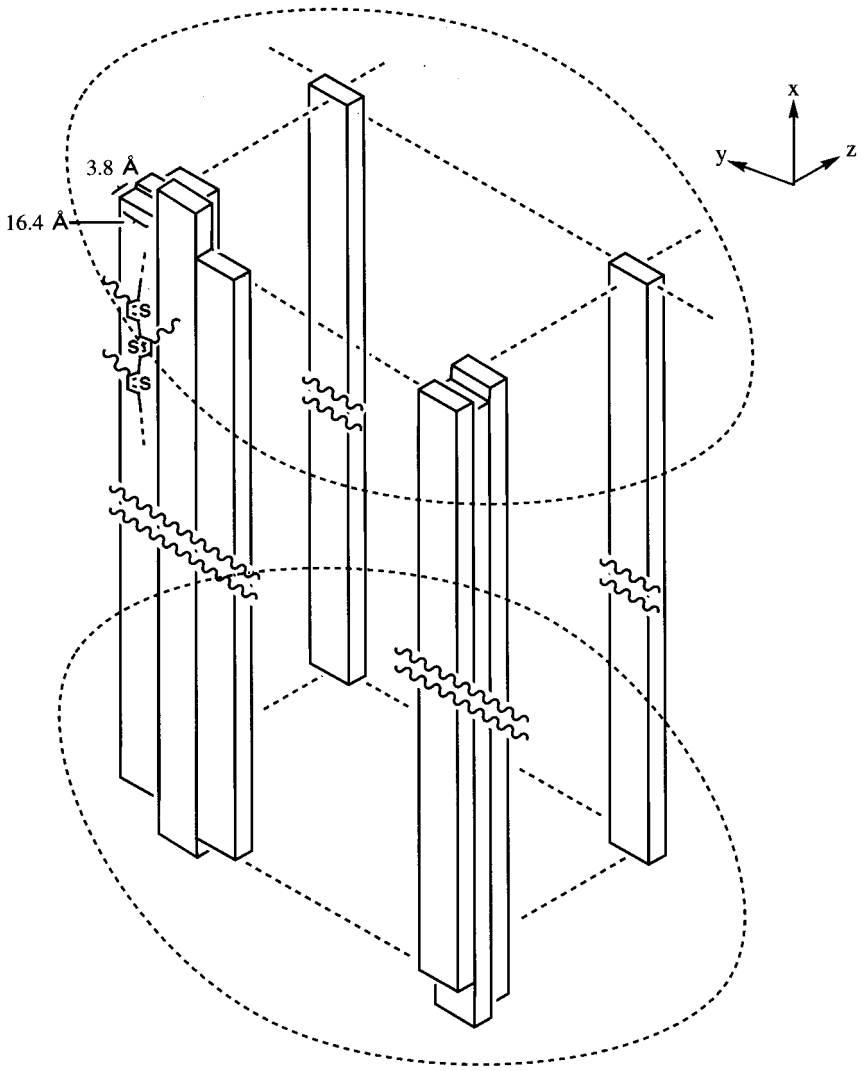

Figure 4. A model for the aggregation of HT-P3HexTh in the colloidal solution; solvent = mixture of $CHCl_3$ and CH_3OH. The aggregate may be consisted of several subunits with the side-to-side stacked molecules.

directions (cf., Figure 4 and Chart 2),[25e] probably by the emergence of mobile electron along the direction of the *y* and *z* axes.

The diameter (vide ante) of the model shown in Figure 4 agrees well with the data shown in part γ in Figure 2, which reveals that the aggregates cannot pass through the pore with a size of 20 nm whereas most of them can pass through the pore with a size of 200 nm.

Deconvolution of the UV−Vis Spectra and Solubility of the Polymer. The UV−vis spectra of the colloidal solution of HT-P3HexTh in the $CHCl_3$−CH_3OH mixtures can be deconvoluted by using the spectrum of HT-P3HexTh in $CHCl_3$ (curve a in the part A in Figure 1) and the spectrum of aggregated HT-P3HexTh (curve i in the part A in Figure 1) as the reference spectra.

For example, the curve c in the part A in Figure 1 is deconvoluted into 47% of curve a and 53% of curve i. In addition, the UV−vis spectrum obtained after filtration of the colloidal solution of the 80/20 mixture of $CHCl_3$ and CH_3OH through the 0.02 μm membrane (part β in Figure 2) agrees well with 47% of the curve a in Figure 1A. On the basis of these data, the solubility of HT-P3HexTh in the 80/20 and 70/30 $CHCl_3/CH_3OH$ mixtures is estimated at about 7 and 2 mg L^{-1}, the values being much smaller than that in $CHCl_3$ (cf., the Supporting Information).

Alignment of P3HexTh in a Stretched PET Film and Transition Moment. Dichroism of π-conjugated polymer in a stretched polymer film (e.g., polypyridine in a stretched poly(vinyl alcohol) film) gives important information about the transition moment of the $\pi-\pi^*$ absorption band of the π-conjugated polymers.[24a,28a]

A PET (poly(ethylene terephthalate)) film containing P3HexTh is obtained by painting the PET film with a $CHCl_3$ solution of P3HexTh followed by drying, and the PET film is stretched. To the stretched film, polarized light is irradiated[28a] to observed the dichroism shown in Figure 5. The stretching ratio R_s and dichroic ratio R_d in Figure 5 are defined as reported previously.[28a]

The PET-P3HexTh films give the following optical results:

(i) HT-P3HexTh easily forms the stacked structure during evaporation of $CHCl_3$ from its $CHCl_3$ solution on the surface of the PET film. PET film thus prepared gives rise to an absorption spectrum characteristic of the stacked HT-P3HexTh. Since the tendency toward the stacking is very strong, even casting a homogeneous $CHCl_3$ solution containing PMMA (poly(methyl methacrylate)) and HT-P3HexTh in a 100:1 ratio on a glass substrate and evaporation of $CHCl_3$ gives a PMMA film containing HT-P3HexTh in the stacked state, as manifested from its UV−vis spectrum.

(ii) On the other hand, P3HexTh(Fe) does not form the well-stacked structure during the evaporation of $CHCl_3$ on the PET

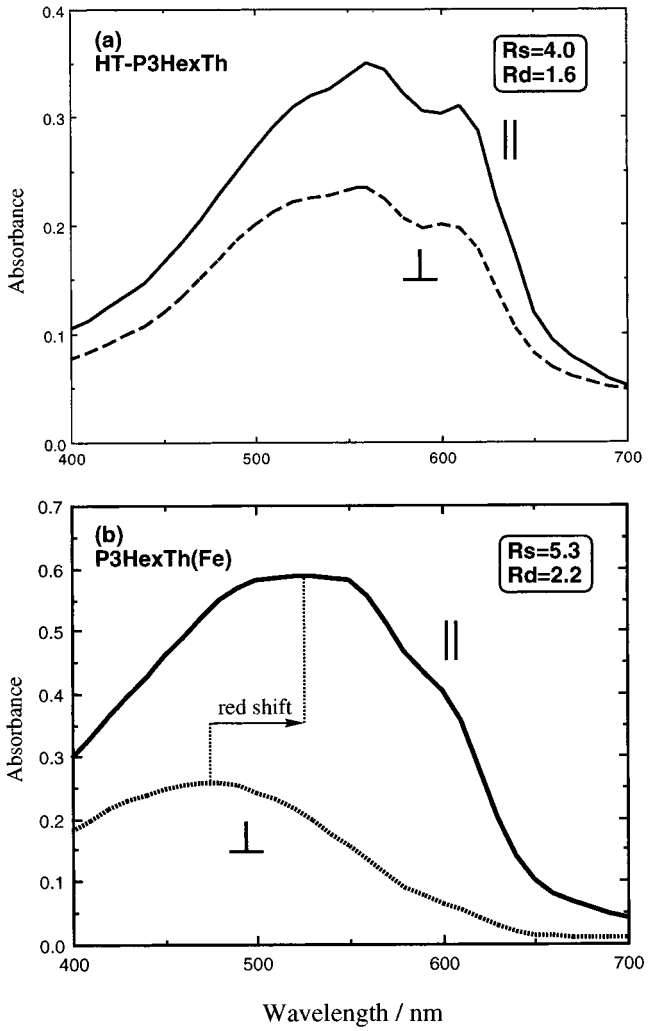

Figure 5. Dichroism of (a) HT-P3HexTh and (b) P3HexTh(Fe) in stretched PET films. The film is irradiated with $h\nu\parallel$ (−) or $h\nu\perp$ (− − − or ···). $h\nu\parallel$ and $h\nu\perp$ stand for polarized light parallel and perpendicular to the direction of the stretching of the PET film, respectively. Definition of the dichroic ratio (R_d) and a stretching ratio (R_s) are given in ref 28a.

film. The film shows a strong absorption band (λ_{max} = 440 nm) of nonstacked P3HexTh(Fe), and only a weak absorption band due to the stacking is observed.

(iii) The stretched PET film containing the stacked HT-P3HexTh shows the dichroism shown in the part a in Figure 5, however, the R_d value is small. This is considered to be due to the difficulty for the stacked large mass to move during the stretching.

(iv) To the contrary, P3HexTh(Fe) gives a larger R_d value (part b in Figure 5). The absorption spectrum observed with $h\nu\perp$ agrees with nonstacked P3HexTh (Fe). On the other hand, the absorption spectrum observed with $h\nu\parallel$ shows a shift of the absorption band characteristic of the stacked state. Moving caused by the stretching will lead to a parallel alignment of the P3HexTh(Fe) molecules and partial stacking through a part suitable to the stacking (presumably a HT-rich micro part; a model is given in the Supporting Information). The data shown in the part b in Figure 5 suggest that the stacked molecule has the transition moment near the direction of the stretching (probably the direction of the main chain of P3HexTh).

Similar π-stacking of a CT-type copolymer (e.g., copolymer of thiophene and quinoxaline)[24a] also takes place on the PET film as judged from a similar bathochromic shift of its λ_{max}, and stretching of the film gives analogous dichroism on the stretched PET film.

Photoluminescence of P3HexTh in the Neat Film and in the Stretched PET Film. Cast films of HT-P3HexTh, P3HexTh (Fe), and P3HexTh (Ni) on glass plates themselves exhibit photoluminescence peaks (λph) at the onsets of their absorption bands (λph = 650, 633, and 593 nm, respectively), as usually observed with π-conjugated aromatic compounds. The excitation spectrum of the pristine neat film of HT-P3HexTh monitored at 650 nm (λph) shows two peaks at 420 and 569 nm, which correspond to the absorption by single HT-P3HexTh molecule and HT-P3HexTh in the stacked state, respectively. These results indicate that the photoenergy absorbed by the single HT-P3HexTh molecule is transferred to an excited state of the assembled mass and is emitted from the mass. On the other hand, the photoenergy absorbed at 569 nm by the assembled mass is normally emitted at the onset (650 nm) of its absorption band.

Examination of dichroism of the photoluminescence with the stretched PET film containing HT-P3HexTh (R_s = 4.0) or P3HexTh(Fe) (R_s = 5.3) (Figure 5) reveals that the strongest photoluminescence is observed at a ∥−∥ (direction of the oscillating electric field of the irradiated light (520 nm) = parallel to the direction of the stretching; the same direction for the emitted light (650 nm)) mode. The intensity of the emitted light measured at other modes (∥−⊥ and ⊥−⊥ modes) is much weaker (less than 10%), suggesting that the photoluminescence also has a transition moment along the direction of the stretching (presumably along the direction of the main chain of P3HexTh or the *x* axis in Figure 4).

Packing Mode of Regioregular P3RThs and P4RTzs in the Solid. X-ray Diffraction. Figure 6 compares powder X-ray diffraction patterns of HT-P3RThs, HH-P4RTzs,[11] *rand*-P4MeTz,[11] and *rand*-P3MeTh prepared by using Mg and Ni.[14]

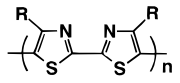

HH-P4RTz

R = CH_3 (HH-P4MeTz)
R = *n*-C_4H_9 (HH-P4BuTz)
R = *n*-C_7H_{15} (HH-P4HepTz)

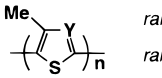

rand-P4MeTz (Y = N; HT/HH = 3/7)[11]
rand-P3MeTh (Y = CH; HT/HH = 4/6)[14,38]

In addition to these previously reported polymers, the following polymers (eqs 1 and 2) have been prepared by using a Stille reaction,[3d,24a,39] and X-ray data of these polymers are also shown in Figure 6. Preparation of regioregular 3-substituted poly(thiophene-2,5-diyl) by a method similar to that expressed by eq 1 has been reported by McCullough and co-workers.[3d]

As shown in Figure 6, HT-P3RThs (except for HT-P3MeTh) and HH-P4RTzs give rise to analogous X-ray diffraction patterns with a peak at a low angle region (θ = ca. 3−13°) and a peak

(36) Newman, S.; Krigbaum, W. R.; Laugier, C.; Flory, P. J. *J. Polymer Sci.* **1954**, *14*, 451.
(37) Bori, K. A.; Sliemrs, F. A.; Stickney, P. S. *J. Polym. Sci. A-2* **1968**, *6*, 1579.
(38) *rand*-P3MeTh gives rise to two peaks for the Me group at δ 2.40 (HT) and 2.21 (HH) ppm in $CDCl_3$.[14] Of the two peaks, HT-P3MeTh (eq 1) shows only one peak at δ 2.42 ppm. From the NMR data, the HT/HH ratio for *rand*-P3MeTh is evaluated. The observation of the HT-CH_3 signal at a lower magnetic field agrees with a general trend observed with P3RTh and P4RTz.[3−11]
(39) (a) Echavarren, A. M.; Stille, J. K. *J. Am. Chem. Soc.* **1987**, *109*, 5478. (b) Kanbara, T.; Miyazaki, Y.; Yamamoto, T. *Polym. Sci., Part A: Polym. Chem.* **1995**, *33*, 999. (c) Wright, M. E.; Porsch, M. J.. Buckley, C.; Cochran, B. B. *J. Am. Chem. Soc.* **1997**, *119*, 8393.

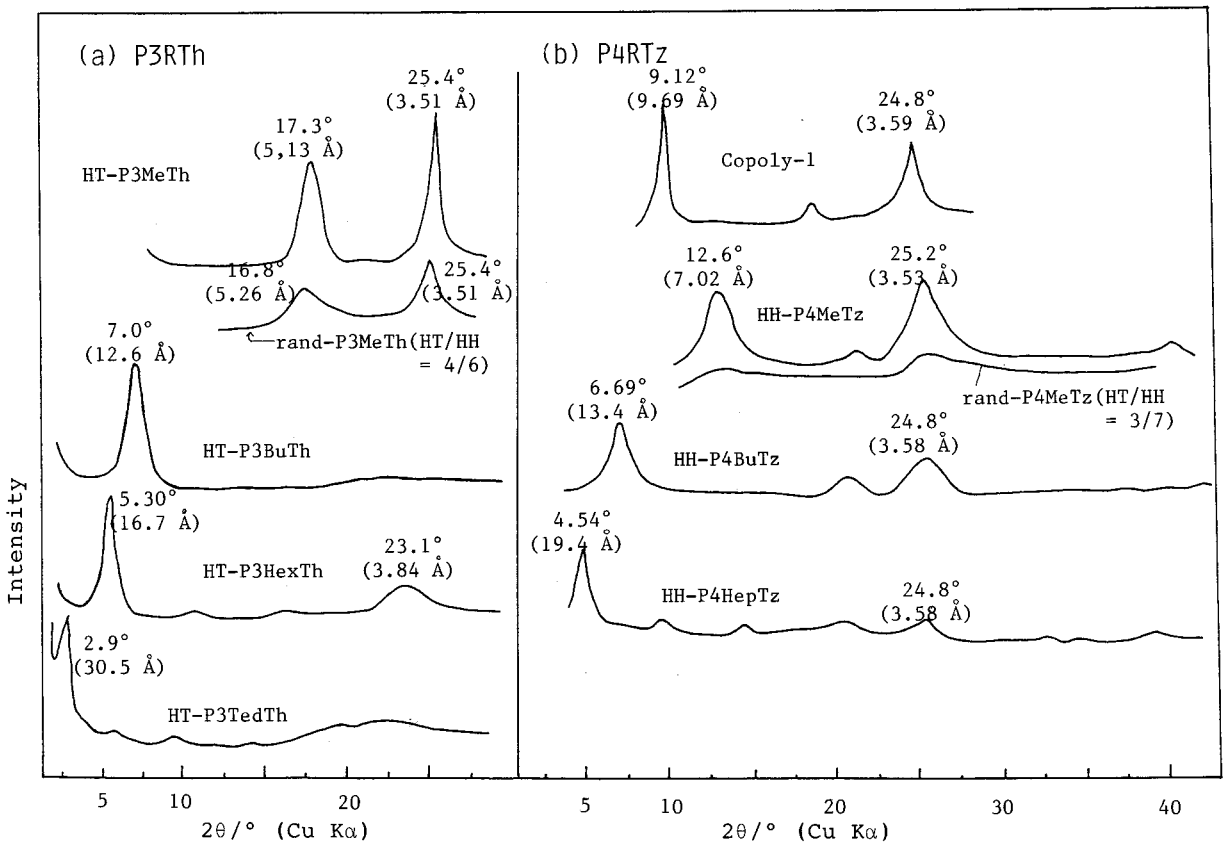

Figure 6. Powder X-ray diffraction patterns of P3RThs and P4RTzs. Data for HT-P3BuTh and HT-P3TedTh (Ted = tetradecyl) are from ref 4a. Other HT-P3RThs, except for HT-P3MeTh, give analogous X-ray diffraction pattern.[3,4]

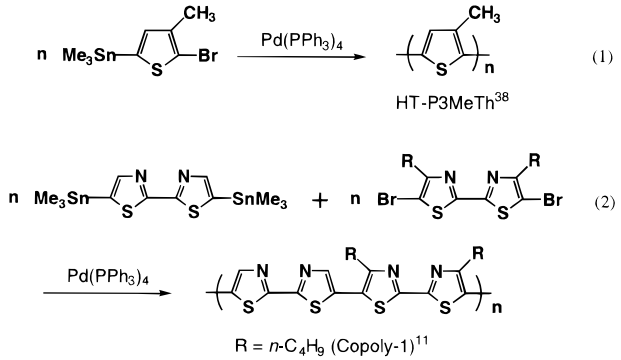

at about $2\theta = 23-25°$. The latter peak at about $2\theta = 23-25°$ is assigned to the face-to-face distance in the stacked molecules (Chart 3 and Figure 4).

The following packing models can be proposed from the X-ray diffraction data.

Model for End-to-end Packing. HT-P3RThs and HH-P4RTzs are considered to have the following s-trans main chain structure, which has been confirmed for low molecular model compounds by single-crystal X-ray analysis.[1c,g,32,33]

CPK molecular models as well as X-ray crystallographic data of a model compound (trimer and tetramer of 3-methylthiophene)[1g,40] indicate that the polymers have a repeating height of about 7.5 Å and the *n*-alkyl chain tilted with θ = about 50° (Chart 5). These data give a distance (D) of about 5.7 Å between the neighboring alkyl chains.

For the packing mode of polymers with alkyl side chains, the following two modes are known (Chart 6) and the number

Chart 5. Structure of HT-P3RTh and HH-P4RTz

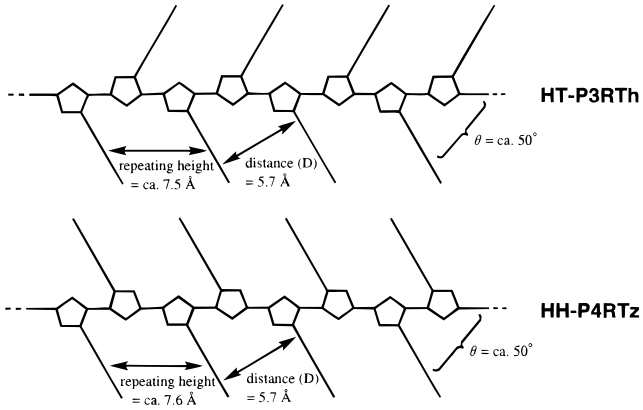

density of the alkyl chain determines the mode of the packing.[12,41,42] In Chart 6, only interaction between two polymer chains is shown. The polymer also has alkyl chains on the other side to form the stacked structure like that depicted in Figure 4. In this chart, the alkyl chains are tilted against the rigid main chain following the models depicted in Chart 5.

The *n*-alkyl group has an effective cross section of 18.4 Å^2 and an effective radius of about 5 Å in crystalline *n*-paraffin and polyethylene[12,43,44] and will take somewhat larger space in the somewhat disordered state. In view of the effective radius

(40) Barbarella, G.; Zambianchi, M.; Bongini, A.; Antolini, L. *Adv. Mater.* **1994**, *6*, 561.

(41) (a) Jordan, E. F., Jr.; Feldeisen, D. W.; Wrigley, A. N. *J. Polym. Sci. Part A-1* **1971**, *9*, 1835.

(42) Hsieh, H. W.; Post, B.; Morawetz, H. *J. Polym. Sci.; Polym. Phys. Educ.* **1976**, *14*, 1241.

(43) (a) Miller, R. L. *High Polymers Vol. XX*; Mark, H., Flory, P. J., Marvel, C. S., Melville, H. W., Eds.; Interscience: New York, 1965; p 585.

(44) Swan, P. R. *J. Polym. Sci.* **1962**, *56*, 403.

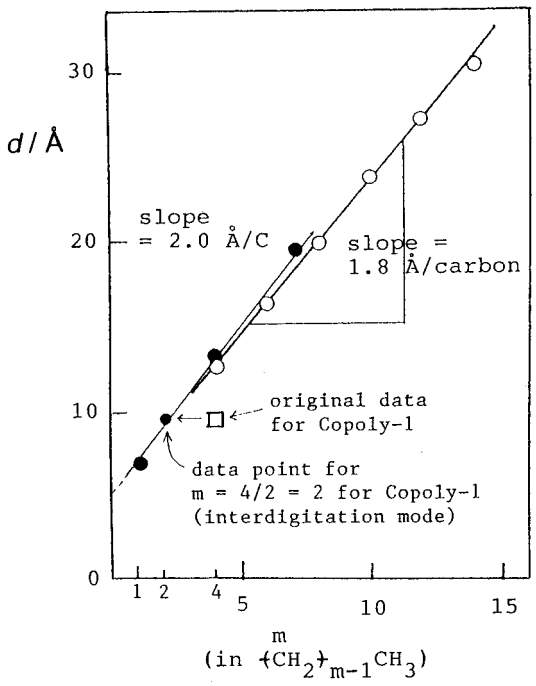

Figure 7. Plots of *d*-spacing between the main chains (Chart 6) against the number of carbons (*m*) in the alkyl side chain (C_mH_{2m+1}) for HT-P3RThs (○) and HH-P4RTzs (●). Data for HT-P3RThs from $m = 4$ (R = *n*-C_4H_9 (Bu)) to $m = 14$ (R = *n*-$C_{14}H_{29}$)(Ted) are from refs 3 and 4.

Chart 6. (a) Interdigitation Model and (b) End-to-End Model for Polymers with Side Alkyl Chains

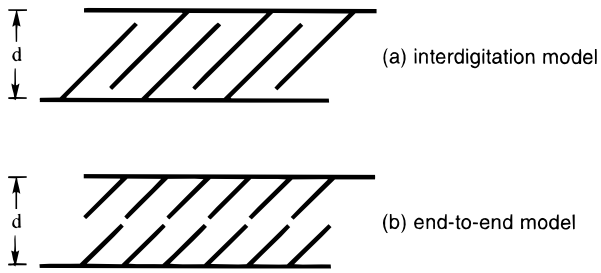

(5 Å) of the alkyl chain and the distance *D* (about 5.7 Å, cf., Chart 5) between the alkyl chains in HT-P3RTh and HH-P4RTz, the polymers are considered to be packed in the end-to-end mode.

Actually plots of the *d*-spacing (Chart 6) estimated from the X-ray diffraction[3,4] against the number of carbon (*m* in the alkyl group $(CH_2)_{m-1}CH_3$) give a linear line with a slope of 1.8−2.0 Å per 1 carbon as depicted in Figure 7. Since the unit height of the alkyl chain per carbon (the CH_2-CH_2 distance along the direction of the alkyl chain) is 1.25 Å,[12,41−44] the interdigitation model gives a slope of less than 1.25 Å because of the tilting of the alkyl chain. For example, a slope of about 0.95 Å per carbon has been observed for poly(aromatic ester)s with alkoxy side chains which are considered to take the interdigitation packing mode.[12d]

In comparison with the interdigitation model, the end-to-end model can give a double slope per the carbon, and the observed slope of 1.8−2.0 Å per carbon is reasonable in view of the tilt angle and the unit height of the alkyl chain: $2 \times 1.25 \times \sin 50° = 1.9$ Å. These data clearly indicate the end-to-end type packing of HT-P3RThs and HH-P4RTzs; however, the packing mode is somewhat different from that proposed for HT-P3RThs previously.[3,4]

Chart 7. Face-Centered Lattice of HT-P3MeTh Where *c*-Axis Is the Direction of the Polymer Chain

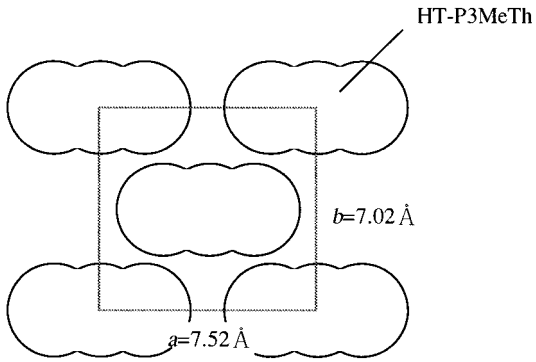

The X-ray diffraction data shown in Figures 6 and 7 further reveal the following features for the stacking of the polymers.

(i) Copoly-1 contains the side alkyl chain in a half density; consequently, Copoly-1 is expected to be packed well in the interdigitation mode. In the interdigitation mode, the effective

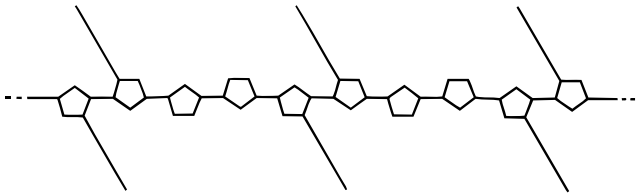

length of the alkyl chain may be estimated at about half of that evaluated for the end-to-end model. Actually, the data point for Copoly-1 in Figure 7 falls on the line for HH-P4RTzs at $m = 4/2 = 2$. The X-ray diffraction data of Copoly-1 can also be interpreted as follows: From the intercept of the line in Figure 7, an effective core size of the main chain is estimated at 5.5 Å. Therefore, an effective length of the butyl group along the direction between the neighboring two polymer chains is calculated as (13.4−5.5)/2 = ca. 4 Å from the X-ray data of HH-P4BuTz. These results yield the *d*-spacing of about 9.5 Å (=5.5 Å + 4 Å) for the interdigitation mode for Copoly-1, which agrees with the observed X-ray data.

(ii) HT-P3MeTh gives a considerably smaller packing distance (3.51 Å) compared with those (ca. 3.8 Å) of HT-P3RThs with longer R chains. The X-ray diffraction data of HT-P3MeTh are reasonably accounted for by the following face-centered lattice type packing mode (Chart 7).

The 3-methylthiophene-2,5-diyl units are considered to take the staggered structure, and the diffractions at $d = 5.13$ and 3.51 Å correspond to 110 and 020 reflections, respectively. The observed layer distance, 3.51 Å, is near that of graphite which also takes a staggered structure.

rand-P3MeTh seems to have an analogous packing mode; however, the diffraction peaks are broadened and the 110 diffraction peak is shifted to a longer *d*-space (5.26 Å, Figure 6). These results are reasonably accounted for by coexistence of lattices with various *a* values (Chart 7) due to certain disorder along the direction of the *a* axis. A simulated X-ray diffraction pattern obtained by taking account of such a disorder agrees with the observed X-ray diffraction pattern in a range of $2\theta = 5-60°$, and detailed results will be reported elsewhere.

(iii) In contrast to HT-P3MeTh, HH-P4MeTz forms the face-to-face packed structure,[11] and its film shows a bathochromic shift characteristic of the face-to-face packing.[11a]

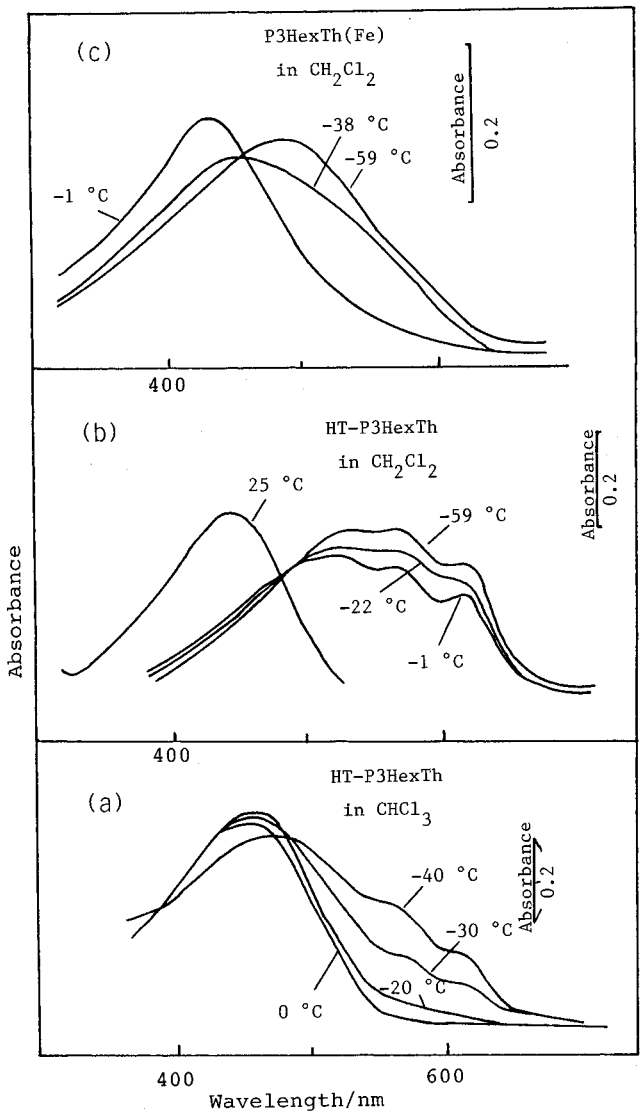

Figure 8. Temperature dependence of UV−vis spectra of (a) HT-P3HexTh in $CHCl_3$, (b) HT-P3HexTh in CH_2Cl_2, and (c) P3HexTh (Fe) in CH_2Cl_2.

(iv) To the contrary, due to the staggered packing structure, the interchain $\pi-\pi$ interaction in HT-P3MeTh is considered to be weak, and the color of solid P3MeThs is almost the same as that of $CHCl_3$ solutions of P3MeThs. Absorption peaks of P3MeThs (ca. 420 nm) in the solid estimated from their reflection spectra and Kramers−Kronig transformation also roughly agree with those of the $CHCl_3$ solutions of P3MeThs. The difference in the presence or absence of the bathochromic shift between HT-P3MeTh and HH-P4MeTz in the solid also support the importance of the face-to-face packing for the bathochromic shift.

(v) HT-P3HexTh has a density of 1.14 g cm^{-3}, which is reasonable for the proposed structure shown in Figure 4 and Chart 3; the proposed structure gives a calculated density of 1.18 g cm^{-3}, and polymer usually shows somewhat lower density than the calculated value due to containing amorphous parts. Less crystalline P3HexTh(Fe) gives a density of 1.09 g cm^{-3}. A high density of HT-P3MeTh (1.47 g cm^{-3}) is also reasonable for the structure shown in Chart 7 (calculated value = 1.53 g cm^{-3}) with the shorter layer-to-layer distance. *rand*-P3MeTh has a lower density of 1.33 g cm^{-3}.

Stacking at Low Temperature and NMR Analysis. Figure 8 exhibits temperature dependence of the UV−vis spectra of P3HexThs. The change of the UV−vis spectrum of the $CHCl_3$ solution of HT-P3HexTh shown in the part a of Figure 8 is similar to that observed on addition of CH_3OH to the $CHCl_3$ solution (Figure 1), and the data support that HT-P3HexTh partly forms the stacked structure at the low temperatures. The ease of the stacking seems to depend on the kind of solvent, and in CH_2Cl_2 (cf., the Supporting Information for the solubility), the stacking takes place more easily at the low temperatures (part b in Figure 8). P3HexTh (Fe) also gives temperature-dependent changes of the UV−vis spectrum (part c in Figure 8) similar to those caused by the addition of CH_3OH (part B in Figure 1). The change of the UV−vis spectrum by lowering the temperature is very small for a CH_2Cl_2 solution of P3HexTh(Ni),[9a] reflecting the low tendency of the polymer to stack.

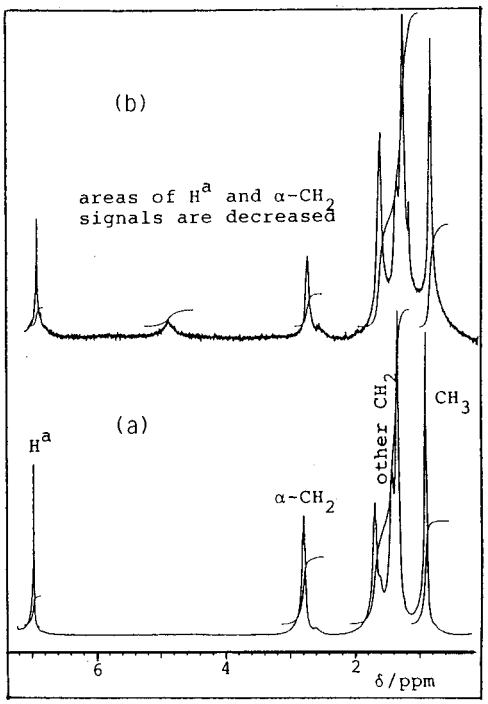

Figure 9. ^1H NMR spectra of HT-P3HexTh in $CDCl_3$ at (a) 0 °C and (b) −20 °C. The small peak at about δ 5.0 ppm is assigned to H_2O contained in the solvent.

By deconvolution of the UV−vis spectra at low temperatures in a manner similar to that applied to the $CHCl_3-CH_3OH$ colloidal solutions, solubility of HT-P3HexTh is estimated at 8.7, 8.2, 6.9, and 2.8 mg L^{-1} at 0, −20, −30, and −40 °C, respectively, from which dissolution enthalpy at the low temperature is roughly obtained as 8 kJ mol^{-1}.

Due to the stacking at low temperature, a $CDCl_3$ solution of HT-P3HexTh for an NMR measurement becomes highly viscous, and the ^1H NMR spectrum shows an interesting tempeature dependence as shown in Figure 9.[9a] The intensity of the peaks of hydrogens in the thiophene (Th) ring and the α-CH_2 of the hexyl group attached at the Th ring is weakened at low temperatures, compared with those of other CH_2 groups and CH_3 group, and the intensity of the Th−H and Th−CH_2− peaks decreases to about 32% of a normal intensity at −20 °C. An decrease in spin−spin relaxation time (T_2)[45a] at Th−H and Th−CH_2− by taking the stacking and/or dispersion of the chemical shift under the rigid circumstances explain the decrease in the peak areas. On the other hand, other CH_2 groups seem to have certain motional freedom and give the normal ^1H NMR

(45) (a) Bloemberger, N.; Purcell, E. M.; Pound, R. V. *Phys. Rev.* **1948**, *73*, 679. (b) Ditchfield, R. *Mol. Phys.* **1974**, *27*, 789. (c) Wolineki, K.; Hinton, J. F.; Pulay, P. *J. Am. Chem. Soc.* **1990**, *112*, 8251.

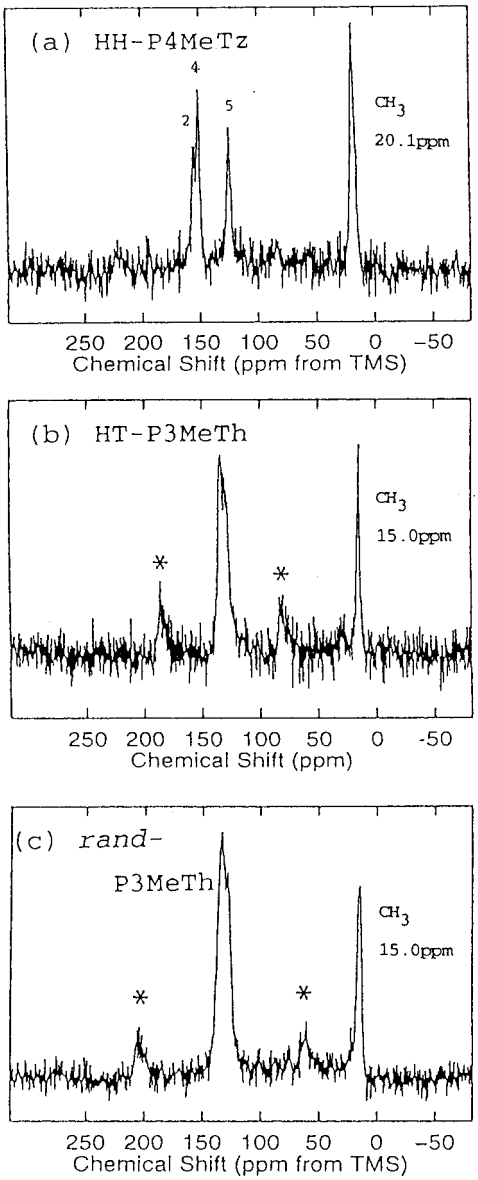

Figure 10. CPMAS solid ^{13}C NMR spectra for (a) HH-P4MeTz, (b) HT-P3MeTh, and (c) *rand*-P3MeTh at 67.94184 MHz. At room temperature. Peaks with an asterisk are due to the spinning sideband of the signal of the aromatic carbons.

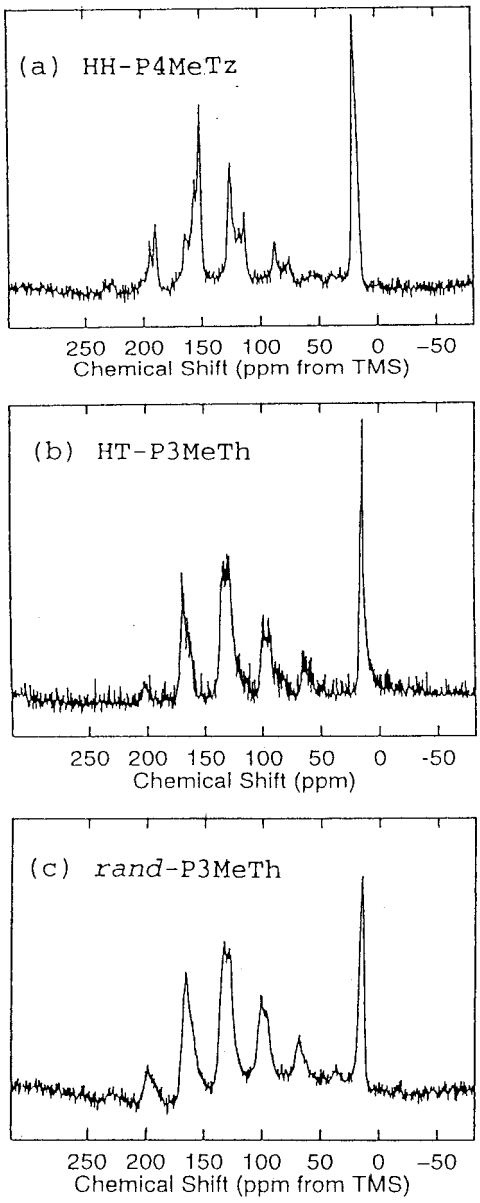

Figure 11. ^{13}C slow spinning CPMAS spectra for (a) HH-P4MeTz, (b) HT-P3MeTh, and (c) *rand*-P3MeTh at 67.94184 MHz. The magic angle spinning rate = 2.5, 2.0, and 2.0 kHz for HH-P4MeTz, HT-P3MeTh, and *rand*-P3MeTh, respectively.

signals. The ^1H NMR spectrum of a dilute solution of P3HexTh(Ni) gives a normal absorption pattern at the low temperatures.

CPMAS Solid ^{13}C NMR Data of HH-P4**MeTz, HT-P3MeTh, and *rand*-P3MeTh.** Figure 10 exhibits the CPMAS solid ^{13}C NMR[45a] spectra for HH-P4MeTz, HT-P3MeTh, and *rand*-P3MeTh at about 67.9 MHz. The four signals of HH-P4MeTz are assigned as depicted below:

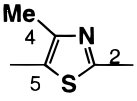

C(2): δ = 155.7 ppm C(5): δ = 126.5 ppm
C(4): δ = 152.2 ppm $C(CH_3)$: δ = 20.1 ppm

The signal assignment has been carried out by chemical shielding calculations based on the coupled Hartree−Fock method with gauge invariant atomic orbital (GIAO-CHF) employing the ab initio 4-31G basis set.[45b,c]

HT-P3MeTh and *rand*-P3MeTh give rise to analogous ^{13}C NMR spectra to each other; however, the half width (264 Hz) of the CH_3-peak of *rand*-P3MeTh is larger than that (106 Hz) of HT-P3MeTh due to the irregular solid structure of the former polymer. Severe overlapping of the signals of aromatic carbons has prevented us from assigning the signals of the aromatic carbons.

The appearance of the Me signal of HT-P3MeTh (δ 15.0 ppm) at a higher magnetic field than that of HH-P4MeTz (δ 20.1 ppm) is associated with the two different packing modes of the two polymers: the staggered packing mode for HT-P3MeTh (Chart 7) and the face-to-face eclipsed packing mode for HH-P4MeTz.[11] The Me carbon in HH-P4MeTz will receive a stronger anisotropic paramagnetism from the other two thiazole rings sandwiching the thiazole ring than that in HT-P3MeTh, thus giving the peak at the lower magnetic field.

A ^{13}C slow-spinning CPMAS measurement gives principal components of the chemical shift tensor,[46, 47] and the principal

(46) (a) Saito, H.; Ando, I. *Ann. Rep. NMR Spectrosc.* **1989**, *21*, 209. (b) Stejskal, E. O.; Schaefer, J.; Waugh, J. S. *J. Magn. Reson.* **1977**, *28*, 105.

(47) Herzfeld, J.; Berger, A. *J. Chem. Phys.* **1980**, *73*, 6021.

Table 1. Principal Components of the Chemical Shift Tensor Estimated from Intensities of MAS Spinning Sidebands

nucleus	δ_{11}	δ_{22}	δ_{33}	δ^a
C(2)	225.6	164.6	76.8	155.7
C(4)	239.5	133.9	83.1	152.2
C(5)	193.1	127.0	59.6	126.5

[a] $\delta = (\delta_{11} + \delta_{22} + \delta_{33})/3$, which agrees with the δ value observed in Figure 10.

components for aromatic carbons of HH-P4MeTz evaluated from the measurement at various spinning rates (e.g., 2.5 kHz for Figure 11a) are summarized in Table 1.

Conclusion and Scope

Data from the light scattering analysis, filtration examination, deconvolution of the UV−vis spectrum, and NMR analysis of the solution and solid reveal the conditions for the π-stacking and the π-stacked structures of the regioregular stiff HT-P3RThs and HH-P4RTzs. Comparison of the data with those of the regioirregular polymers supports the obtained conclusion. X-ray diffraction analysis indicates that HT-P3RThs and HH-P4RTzs take the π-stacked structure with the end-to-end packing mode. On the other hand, Copoly-1 with the side alkyl chain in a half density is packed in the interdigitation style. HT-P3MeTh takes the face-centered lattice in the solid, and UV−vis data as well as CPMAS solid ^{13}C NMR data agree with the solid structure. The stacked HT-P3HexTh molecules show the photoinduced polarizability not only along the polymer main chain but also along the other two directions; however, the transition moments of the UV−vis absorption and photoluminescence are considered to be along the polymer main chain. As reported in this paper, π-stacking of linear π-conjugated polymers is susceptible to various physical chemical analyses, and the obtained data provide interesting information about the π-stacking. Extension of the investigation is expected to give important informations not only for polymer chemistry but also for organic chemistry, biochemistry, and material chemistry.

Experimental Section

Materials. P4RTzs,[11] P3HexTh(Fe),[20] P3HexTh(Ni),[26] *rand*-P3MeTh,[14] and Copoly-1[11] were prepared as previously reported. HT-P3HexTh and HT-P3DodTh were purchased from Rieke Metals, Inc. Whatman biofilters were used for filtration of the colloidal solutions. Unstretched PET film was kindly donated from Toyobo Co., Ltd. HT-P3MeTh was prepared from 2-bromo-5-(trimethylstannyl)-3-methylthiophene, Me_3Sn-MeTh-Br, by use of the Stille reaction developed by McCullough and co-workers (eq 1).[3d] 2-Bromo-3-methylthiophene was prepared according to the literature,[48] and the compound was treated with lithium diisopropylamide at −70 °C. To the reaction mixture was added Me_3SnCl, and 1 h of stirring at −50 °C followed by distillation (66−67 °C/1.5−1.7 mmHg) gave colorless Me_3Sn-MeTh-Br in 69% yield. Anal. Found: C, 28.3; H, 3.7. Calcd: C, 28.3; H, 3.9. ^{1}H NMR (DMSO-d_6): δ 0.32 (9H), 2.13 (3H), 6.95 (1H). Polymerization was carried out in dry DMF at 85 °C with $Pd(PPh_3)_4$.

Measurements. Measurements of UV−vis and photoluminescence spectra including their anisotropy,[28a] X-ray diffractometry,[11,12a,b] and NMR analysis for solutions[28a] were carried out in manners similar to those previously reported. The light scattering analyses[25a,b] were carried out by using He−Ne laser at 25 °C. The wavelength of the incident beam was 632.8 nm in a vacuum. For the determination of the degree of depolarization (ρ_v), it was used for the scattering geometry that vertically polarized incident beam was irradiated and intensities of the vertically (V_v) and horizontally (H_v) scattered light were detected. To take account of the angular dependence of the scattered light intensity, the extrapolated values to zero scattering angle were used for the analysis of the optical anisotropy of P3HexTh, $\rho_v = H_v/V_v$. CPMAS solid ^{13}C NMR spectra were recorded on a JEOL GSX-270 NMR spectrometer equipped with a CPMAS probe. The density of the polymer was determined by sink and floot tests.

Acknowledgment. We are grateful to Professor Y. Morooka, Professor K. Osakada, Dr. K. Fujisawa, Mr. T. Maruyama, and Mr. I. Yamaguchi of our institute for their helpful discussions and experimental support. This work has been partly supported by a Grant-in-Aid for Science Research (priority area "polymer nano-structure") from the Ministry of Education, Science, Sports, and Culture and by CREST (Core Research for Evolutional Science and Technology).

Supporting Information Available: Solubility of HT-P3HexTh, UV−vis data of P3RThs and HH-P4BuTz, and a model for stacking of P3HexTh (Fe) during the stretching of the PET film (3 pages). See any current masthead page for ordering information and Web access instructions.

JA973873A

(48) Diffmer, K.; Martin, R. P.; Herz, W.; Cristal, S. I. *J. Am. Chem. Soc.* **1949**, *71*, 1201.